

Automated Layout Design and Control of Robust Cooperative Grasped-Load Aerial Transportation Systems

Carlo Bosio, Jerry Tang, Ting-Hao Wang, and Mark W. Mueller

Abstract— We present a novel approach to cooperative aerial transportation through a team of quadcopters, using optimal control theory and a hierarchical control strategy. We assume the quadcopters are connected to the payload through rigid attachments, essentially transforming the whole system into a larger flying object with “thrust modules” at the attachment locations of the quadcopters. We investigate the optimal arrangement of the thrust modules around the payload, so that the resulting system is robust to disturbances. We choose the \mathcal{H}_2 norm as a metric of robustness, and propose an iterative optimization routine to compute the optimal layout of the vehicles around the object. We experimentally validate our approach using four quadcopters and comparing the disturbance rejection performances achieved by two different layouts (the optimal one and a sub-optimal one), and observe that the results match our predictions.

I. INTRODUCTION

The growing demand for effective and autonomous transportation in applications such as logistics, search and rescue operations, and load lifting has increased interests in efficient aerial transportation solutions [1]. Being able to apply aerial robots to logistics and transportation would not only reduce costs and enhance efficiency, but also allow to reduce the burden on ground infrastructures. The application of UAVs to these fields is challenging, mainly due to their payload and battery life limitations. We address the problem of using multiple quadcopters for payload lifting and transportation. A lot of work has been carried out on design, control and path planning for single quadcopter transportation systems, some examples of which are [2], [3], [4], [5], [6], [7]. However, practical limitations on dimensions, vehicle complexity, load capacity, and costs limit the application of such technologies.

The widespread use and cost-effectiveness of smaller vehicles, such as quadcopters, have made them the preferred choice for practical applications [8]. However, using multiple smaller vehicles in a cooperative manner, along with potential payload interactions (e.g. aerodynamic interactions, vibrations), also introduces greater complexity in terms of control and trajectory planning for cooperative aerial transportation systems [9], [10]. Connecting the vehicles to the payload through tethers is a popular choice, and allows to distance the agents from the payload. The dynamics and control of tethered systems have been extensively investigated and yielded interesting results, e.g. [11]. Other examples are [12], which employed an interconnected structure to

The authors are with the Dept. of Mechanical Engineering, University of California, Berkeley {c.bosio, jerrytang, wtyng, mwm}@berkeley.edu



Fig. 1: Picture of four quadcopters cooperatively carrying a single panel payload.

enhance the stability of the tethered system, or [13], which implemented a decentralized control scheme not relying on assumptions about the payload’s state. [14] presented a cooperative control approach which showed significant disturbance rejection performances. Compared to the challenges of managing tethered or moving payloads, which can be complex due to their internal dynamics and limited maneuverability, rigid attachments are often the preferred option for transportation purposes. Some work has been carried out also along this direction. [15] studied the control for cooperative payload stabilization with a team of quadcopters equipped with grippers. [16] focused on cooperative grasped transportation control using onboard visual and inertial sensing, while [17] implemented an adaptive control framework based on a Kalman Filter for systems with uncertainty about quadcopter location and payload parameters. [18] explores the possibility of transporting flexible payloads, taking into account internal deformations and dynamics and aiming to minimize deformations.

Our research addresses the synthesis of rigidly attached transportation systems. The core concept is to address both the design layout and the optimal control of the combined quadcopter-payload system as one unified problem. We do this by formulating and solving an optimization problem derived from robust control theory for a first order model of the system. In particular, \mathcal{H}_2 control proved to be a promising approach to maximize disturbance rejection performances [19]. The main contribution of this research is an automated design tool to determine the optimal thrust module arrangement for payload stability and robustness. Experimentally validated with four quadcopters, our method confirms the effectiveness of the optimal layout in rejecting disturbances.

The paper is structured as follows. In Section II we describe the mathematical framework employed to compute the optimal placement locations and the linear feedback

law to control the system. We then describe the control infrastructure adopted in our hardware setup. In Section III we show some example outputs of our optimization routine applied to different payload shapes, masses and number of quadcopters used for transportation. In Section IV we introduce the experimental setup and the flight tests which were carried out to validate the theoretical predictions. Finally, in Section V we discuss the results, relevance of the work and future developments.

II. MATERIALS AND METHODS

The problem we solve is twofold. We first optimize the placement of the quadcopters on the object to be transported, so as to maximize the system's disturbance rejection performance. This involves solving an optimization problem where the cost function is derived from \mathcal{H}_2 control theory, and the decision variables are the quadcopters' attachment locations. We then address the constrained quadcopters dynamics through a hierarchical control strategy of the integrated quadcopter-payload system. The motion of the system is controlled using the gain obtained from the same \mathcal{H}_2 control used for layout optimization. Each quadcopter (thrust module) is sent thrust commands. An example picture of a team of quadcopters carrying a payload with rigid attachments is shown in Fig. 1.

A. Modelling

We make the two following key assumptions about our system.

Assumption 1: The payload is characterized by an orthogonal extrusion geometry.

Assumption 2: The payload inertia is fully known. Assumption 1 simplifies the following mathematical derivation, but does not limit significantly the space of possibilities: indeed many objects, such as delivery packages, boxes, and pallets are all included in this category. In such case, we investigate the quadcopters' placement on the mid plane of the extrusion (Fig. 2a)), reducing the size of the optimization problem formulated. The relaxation of this assumption will be a future extension. Assumption 2 simplifies the control infrastructure, and can also be relaxed in the future.

With reference to Fig. 2b), the placement variables, are defined as the angles $\theta = [\theta_1, \dots, \theta_N]^T$ describing the attachments locations along the curve Γ with respect to the centroid of the payload shape. We highlight that this is just a geometric parametrization choice, and no assumption is made on the overall center of gravity of the system. The attachment is assumed to be obtained through a rigid rod, which allows to keep distance between payload and thrust modules.

The quadcopter-payload ensemble is itself a rigid body, and can therefore be described by a state vector $\mathbf{x} = [\mathbf{p}^T, \dot{\mathbf{p}}^T, \boldsymbol{\gamma}^T, \boldsymbol{\omega}^T]^T \in \mathbb{R}^{12}$, where \mathbf{p} and $\dot{\mathbf{p}}$ are the position and velocity of the centroid of the object with respect to a global world reference frame, $\boldsymbol{\gamma}$ is the Roll-Pitch-Yaw triplet defining the orientation of the local frame, and $\boldsymbol{\omega}$

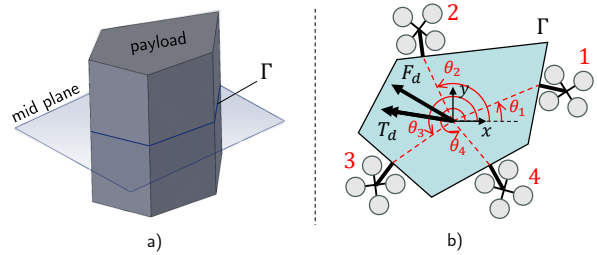


Fig. 2: a) Extrusion payload geometry and representation of the mid-plane. Its intersection with the side faces is the curve Γ . b) Schematics of four quadcopters attached around the payload along Γ . Representation of the local body reference frame centered at the centroid of Γ , placement variables defined by the angles θ_i ($i = 1, \dots, 4$), and disturbance force F_d and torque T_d .

the angular velocity with respect to the local body frame. Tracking the motion of the centroid of the payload rather than the center of mass of the system (which in general do not coincide) is a design choice due to the geometric relevance of the former. As such, our methods would not be impacted by a different definition of the state vector. Each quadcopter is seen as a thrust module providing four inputs to the system. Therefore, if N quadcopters are deployed, the thrust input vector is $4N$ -dimensional, i.e. $\mathbf{u} \in \mathbb{R}^{4N}$. Due to unavoidable hardware limitations, we assume that each thrust component is limited to the interval $[u_l, u_h]$. It is possible to linearize the rigid body dynamics model about hover configuration, and decompose the inputs in $\mathbf{u} = \bar{\mathbf{u}} + \mathbf{u}'$, in which $\bar{\mathbf{u}}$ are the feedforward thrusts and \mathbf{u}' are the first order components of the linearized model. We do the same for the state vector $\mathbf{x} = \bar{\mathbf{x}} + \mathbf{x}'$. We model the disturbances applied to the system as a random variable $\mathbf{d} = [\mathbf{F}_d^T, \mathbf{T}_d^T]^T$, in which $\mathbf{F}_d \in \mathbb{R}^3$ and $\mathbf{T}_d \in \mathbb{R}^3$ represent white noise force and a torque applied to the origin of the local body reference frame. The problem is formulated as the minimization of the probability of infeasible inputs when the system is subject to the defined random disturbance vector $\mathbf{d} \in \mathbb{R}^6$. We analyze the integrated quadcopter-payload system as a whole. We can write its continuous-time linearized dynamics as:

$$\dot{\mathbf{x}}' = A \mathbf{x}' + B(\boldsymbol{\theta}) \mathbf{u}' + B_d(\boldsymbol{\theta}) \mathbf{d}. \quad (1)$$

The dynamics matrix $A \in \mathbb{R}^{12 \times 12}$ is obtained by linearization of the rigid body dynamics equations about hovering and does not depend on the placement variables $\boldsymbol{\theta}$. The matrices $B(\boldsymbol{\theta}) \in \mathbb{R}^{12 \times 4N}$ and $B_d(\boldsymbol{\theta}) \in \mathbb{R}^{12 \times 6}$ depend on $\boldsymbol{\theta}$ either directly or through the inertia of the system (which itself is a function of $\boldsymbol{\theta}$).

B. Layout Optimization

With reference to the \mathcal{H}_2 optimal control literature [20], we define an additional auxiliary variable:

$$\mathbf{z} = C \mathbf{x}' + D \mathbf{u}'. \quad (2)$$

The dimension of \mathbf{z} can vary, and mainly depends on the desired control authority along the directions of interest in the state and input spaces. The goal is to find the feedback

gain K^* such that

$$\mathbf{u} = \bar{\mathbf{u}} - K^*(\boldsymbol{\theta})\mathbf{x}', \quad (3)$$

where $\bar{\mathbf{u}}$ are the feedforward inputs, and minimize the integral \mathcal{H}_2 control cost $J = \sum_{k=1}^6 \left[\int_0^\infty \mathbf{z}^T \mathbf{z} dt \text{ s.t. } \mathbf{d} = \mathbf{e}_k \delta(t) \right]$, where \mathbf{e}_k is the k -th element of the euclidean base, $\delta(t)$ is Dirac's delta function, and the summation upper bound (i.e. 6) is the dimensionality of the disturbance vector \mathbf{d} . It is a known result that the optimal feedback controller is obtained as

$$K^*(\boldsymbol{\theta}) = (D^T D)^{-1} B(\boldsymbol{\theta})^T S_1(\boldsymbol{\theta}) \quad (4)$$

where $S_1(\boldsymbol{\theta})$ is the solution of the algebraic Riccati equation:

$$A^T S_1 + S_1 A - S_1 B (D^T D)^{-1} B^T S_1 + C^T C = 0 \quad (5)$$

in which we omitted the dependency on $\boldsymbol{\theta}$ for clarity of writing. The feedback gain does not depend on the matrix B_d , which represents how the disturbance affects the dynamics. The optimal cost value turns out to be:

$$J^* = \text{tr}(B_d^T S_1 B_d). \quad (6)$$

The optimal cost value does indeed depend on the matrix B_d . This is a valid cost function which can be used to optimize the quadcopters' attachment locations. However, it does not guarantee that the inputs generated by eq. 3 are feasible. Therefore, we make an additional step: we compute the covariance $S_2(\boldsymbol{\theta})$ of the state vector in a condition in which the optimal feedback is active and the system is subject to white noise disturbance. This can be computed using the optimal continuous-time state observer theory, which leads to the equation:

$$A_f S_2 + S_2 A_f^T + B_d B_d^T = 0 \quad (7)$$

where we defined $A_f(\boldsymbol{\theta}) = A - B(\boldsymbol{\theta})K^*(\boldsymbol{\theta})$ as the dynamics matrix with linear feedback. Note that the assumption of white noise disturbance makes the process ergodic, and therefore the state sample mean is equivalent to the temporal mean. The matrix $S_2(\boldsymbol{\theta})$ is then an approximation of the covariance of the first order state linearization \mathbf{x}' when subject to white noise disturbance. At this point we have the feed-forward thrust values, which are computed from the hovering equilibrium condition, and the covariance matrix of the inputs, obtained through the feedback law $K^*(\boldsymbol{\theta})^T S_2(\boldsymbol{\theta}) K^*(\boldsymbol{\theta})$. The goal is to maximize the probability of feasible inputs. If we set the element-wise thrust lower bound to be $\mathbf{u}_l = u_l \mathbf{1}_{4N}$ and the upper bound to be $\mathbf{u}_h = u_h \mathbf{1}_{4N}$, where $\mathbf{1}_{4N}$ indicates the $4N$ -dimensional vector of ones. We can then write the optimization problem we are trying to solve as:

$$\max_{\boldsymbol{\theta}} F(\mathbf{u}_h) - F(\mathbf{u}_l) \quad (8)$$

where $F(\cdot)$ is the cumulative distribution over thrust inputs, and its mean and covariance depend on $\boldsymbol{\theta}$. It is possible to approximate this cumulative distribution through sampling, but the sampling approach would lead to a noisy cost function for our optimization problem, whose variance decreases linearly

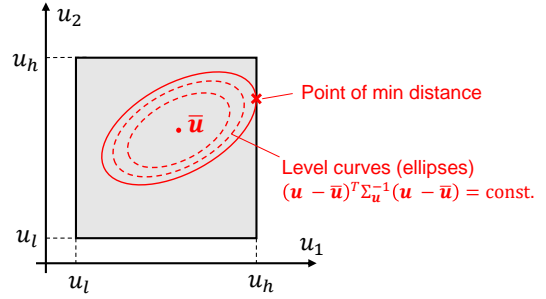


Fig. 3: Two dimensional example of minimum Mahalanobis distance to input bounds. In this case, the random variables are $u_1, u_2 \in [u_l, u_h]$. The ellipses depicted, centered at the mean $\bar{\mathbf{u}}$, represent the level curves of the Mahalanobis distance and are obtained as $(\mathbf{u} - \bar{\mathbf{u}})^T \Sigma_{\mathbf{u}}^{-1} (\mathbf{u} - \bar{\mathbf{u}}) = q$ (q being a positive scalar parameter). The ‘‘point of minimum distance’’ sought is given by the tangency between the largest ellipsoid contained in the bounding box and the corresponding bounding hyperplane.

with the number of samples used. An additional limitation of sampling is that it needs a distribution to draw samples from, and this would have to be assumed. In addition, sampling-based methods are computationally expensive and lead to long solution times. Therefore, we choose to leverage the concept of minimum Mahalanobis distance [21] of the mean (feedforward thrusts) to the thrust bounds. The Mahalanobis distance of a point \mathbf{u} to a distribution with mean $\bar{\mathbf{u}}$ and covariance $\Sigma_{\mathbf{u}}$ is defined as:

$$d_M(\mathbf{u}; \bar{\mathbf{u}}, \Sigma_{\mathbf{u}}) = \sqrt{(\mathbf{u} - \bar{\mathbf{u}})^T \Sigma_{\mathbf{u}}^{-1} (\mathbf{u} - \bar{\mathbf{u}})}. \quad (9)$$

We can extend the concept of Mahalanobis distance to a hyperplane as the minimum Mahalanobis distance of a point of the hyperplane from the distribution. A two dimensional example is shown in Fig. 3. Since in our case we have a lower and an upper bound for each input, and four thrust inputs per quadcopter, there are $8N$ different bounding hyperplanes to consider in the input space. Therefore, going back to the goal of maximizing the probability of feasible inputs, we aim to maximize the Mahalanobis distance of the mean (feedforward thrusts) to the thrust bounds. The optimization problem can be formulated as:

$$\begin{aligned} \max_{\boldsymbol{\theta}} \left\{ \min_k \left[\min_{u_a \in \{u_l, u_h\}} \left(\min_{\mathbf{u}} d_M(\mathbf{u}; \bar{\mathbf{u}}(\boldsymbol{\theta}), \Sigma_{\mathbf{u}}(\boldsymbol{\theta})) \right) \right] \right\} \\ \text{s.t. } \mathbf{u}_l \leq \mathbf{u} \leq \mathbf{u}_h \text{ (element-wise)} \\ u^{(k)} = u_a \end{aligned} \quad (10)$$

In which with the superscript $u^{(k)}$ we refer to the k -th component of the vector \mathbf{u} . We are then dealing with a nested optimization problem. Trying to unpack what the routine is about: we are looking for the value $\boldsymbol{\theta}^*$ which maximizes the minimum Mahalanobis distance of the thrust bounds from the feedforward thrust. This minimum distance is computed by evaluating it on each bounding hyperplane separately, hence the minimization over k (component-wise) and over $u_a \in \{u_l, u_h\}$, where the subscript a stands for ‘‘active’’. The inner minimization over \mathbf{u} is necessary because, on each bounding hyperplane, we are interested in finding the point with minimum distance from $\bar{\mathbf{u}}$. The

optimization routine is also described in Algorithm 1. On the computational cost level, there are no particularly expensive operations. Solving Riccati equations is relatively fast, and minimizing the Mahalanobis distance from a hyperplane is a Quadratic Program (QP). For each update of θ in the optimization routine, $8N$ QPs are solved. The solver used for the outer optimization loop is the Nelder-Mead simplex method discussed in [22] and [23].

Algorithm 1 \mathcal{H}_2 based quadcopter placement optimization

Require: N , quadcopters inertia, object inertia, object shape

Require: weight matrices C and D

Initial guess for θ

while Optimization not completed **do**

 Compute overall system inertia

 Compute A , $B(\theta)$, $B_d(\theta)$ and feedforward $\bar{\mathbf{u}}$

 Compute $S_1(\theta)$ and $K^*(\theta)$ from eq. 5

 Compute $S_2(\theta)$ from eq. 7

 Compute input covariance as $\Sigma_{\mathbf{u}} \leftarrow K^{*T} S_2 K^*$

 Initialize d_M^*

for each thrust input component k **do**

for u_a in $\{u_l, u_h\}$ **do**

 Solve QP $d' \leftarrow \min_{\mathbf{u}} d_M(\mathbf{u}; \bar{\mathbf{u}}, \Sigma_{\mathbf{u}})$ as in eq.

 10 s.t. $\mathbf{u}_l \leq \mathbf{u} \leq \mathbf{u}_h$, $u^{(k)} = u_a$

if $d' < d_M^*$ **then**

$d_M^* \leftarrow d'$

end if

end for

end for

 Update θ (Nelder–Mead simplex algorithm)

end while

C. Control Infrastructure

The dynamics of motion of each quadcopter is highly constrained due to the rigid attachments. Therefore, using a traditional quadcopter controller would be challenging. However the integrated system corresponds itself to a larger rigid body (neglecting effects due to internal elasticity and vibrations). Therefore, approaching the overall dynamics and control as a whole (as was done for the placement optimization) is preferable. This strategy leads to a hierarchical control infrastructure, in which a single estimator is used for the overall motion and the quadcopters receive thrust commands individually through N parallel communication channels. Furthermore, this control strategy comes naturally from the layout optimization computation, during which the optimal LQR gains have been computed. A block diagram of the suggested control infrastructure is shown in Fig. 4. The overall behavior of the controller is dominated by the choice of some parameters which directly impact the computation of the \mathcal{H}_2 cost. First, the disturbance matrix B_d (eq. 1) describing how the random disturbance affects the dynamics, and, in particular, its variance along different directions in the wrench space. Second, the matrices C and D (eq. 2), i.e. how the auxiliary variable z is defined.

For simplicity, the B_d matrix was chosen to weigh the six disturbance components equally, i.e. $B_d(4, 1) = B_d(5, 2) = B_d(6, 3) = B_d(10, 4) = B_d(11, 5) = B_d(12, 6) = 1$. The C matrix is chosen to just weight the position of the payload centroid and the system’s yaw angle (i.e. $C \in \mathbb{R}^{(4+4N) \times 12}$). After evaluating the system’s behavior in simulation, we set $C(1, 1) = C(2, 2) = 0.5$ (corresponding to the position on a horizontal plane $x - y$), $C(3, 3) = 10$ (corresponding to vertical position z), $C(4, 9) = 50$ (corresponding to yaw angle), and zero for all the other components. The input weight matrix $D \in \mathbb{R}^{(4+4N) \times 4N}$ was set to the block matrix $D = [\mathbf{0}_{4N \times 4}, I_{4N}]^T$, where $\mathbf{0}_{m \times n}$ denotes the $m \times n$ matrix of all zero elements and I_k the k -dimensional identity.

D. Hardware Setup

The vehicles we used as a reference for layout design and eventually for experiments are quadcopters equipped with a PX-4 flight controller. The relevant vehicle parameters can be found in Tab. I. The battery capacity (5300 mAh)

quadcopter size (motor to motor)	330 mm	propeller diameter	114.5 mm
quadcopter frame mass	525 g	battery mass	437 g

TABLE I: Table of parameters

has been chosen to guarantee 10 minutes of flight time at maximum payload. The system theoretically is able to lift an external payload of ~ 0.8 kg per quadcopter. It is interesting to note that the main contribution to the overall inertia of the system is due to the quadcopters, since they are attached to the payload perimeter, and thus at a larger distance from the overall center of mass. It is interesting to highlight that contributing a greater inertia than the actual payload transported is in line with all the ground and aerial transportation systems in use nowadays.

III. RESULTS

The optimization framework which we developed allows us to determine the optimal placement of quadcopters for transportation across many different payload shapes, mass values and number of quadcopters used. In Fig. 5 we show some examples of optimal placements using the vehicles described in Tab. I as a reference. It is interesting to observe that the quadcopters are placed in a way which seems to trade off two different contributions. On the one hand, the area of the polygon defined by the quadcopters’ attachment points tends to be maximized in order to maximize control authority. On the other hand the distances of the attachment points to the system’s center of mass tend to be equalized. This is an effect of employing the Mahalanobis distance as a metric. In fact, even if the control authority is maximized (i.e. the input covariance $\Sigma_{\mathbf{u}}$ has smaller eigenvalues), we also need the quadcopters to have a comparable margin between feedforward thrusts $\bar{\mathbf{u}}$ and bounds, otherwise the Mahalanobis distance objective is decreased.

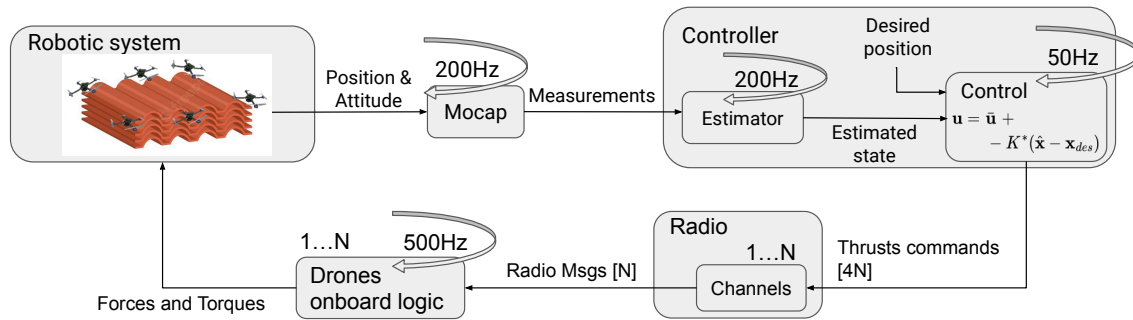


Fig. 4: Control infrastructure diagram

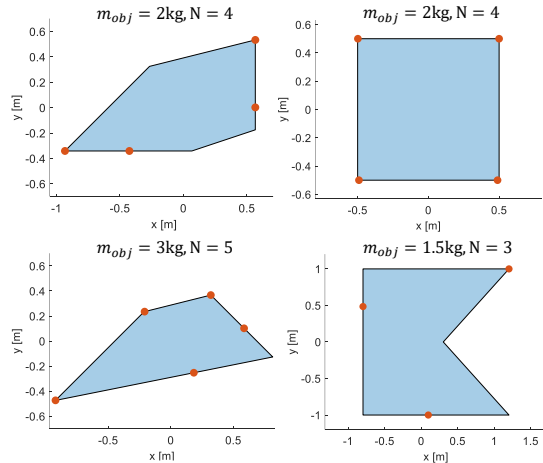


Fig. 5: Optimal layouts for various object shapes and masses using different number of quadcopters. Our approach can handle both convex and non-convex polygons. It is interesting to note that, in contrast to common intuition, the optimal drone placement around a symmetric shape might not be symmetric as well.

IV. EXPERIMENTAL VALIDATION

For the flight experiments the quadcopters were attached to two different square panels of different masses and sizes. A heavier panel (A) of side length 0.61 m and mass 2.54 kg was used to test the payload capacity, and a lighter one (B) of side length 0.45 m and mass 1.088 kg to test the disturbance rejection performances. The rigid attachments have been obtained by screwing directly the quadcopters to the panels through wood dowels. The experiments are conducted in an indoor flight space equipped with a Motion Capture system, and markers for motion tracking are placed directly on the panels.

A. Payload lifting

Panel A was used to test the payload capacity of the system. The four quadcopters were attached to the corners of the panel and a hovering position was commanded. The system was able to successfully take off, stabilize, hover and land safely. An important observation to highlight is the close proximity of the feedforward thrusts \bar{u} to the upper thrust limit u_h . Given the significant mass of Panel A (~ 2.5 kg) compared to the quadcopter masses (~ 0.95 kg

including battery), the narrow margin causes the system to have limited disturbance response capabilities, especially within the spatial limits of the flight space available for experiments.

B. Disturbance Rejection

The four quadcopters were attached to panel B using two distinct configurations: an optimal one, placed at the corners, and a sub-optimal one. These configurations can be seen in Fig. 6. As a disturbance, a weight of 0.5 kg, or approximately 10% of the system's total mass, was attached to a corner of the panel during the flight, specifically under Quadcopter 1 (Fig. 6). The mass attachment is done through a magnet to guarantee the repeatability of the experiment. Both the state and input data were collected and compared to validate their consistency with the layout optimization framework. Representative response plots over time are presented in Fig. 7.

From the data, it is clear that the choice of quadcopter layout has a significant impact on disturbance rejection performance. The optimal layout results in lower oscillations in the attitude of the vehicle, specifically in the pitch and roll angles, and also recovers more quickly from disturbances. In comparison, the sub-optimal layout sees its peak deviation from hovering conditions nearly double the one of the optimal setup. Another observation is related to thrust behavior after adding the payload. In the sub-optimal configuration, the increase in thrust following the addition of the payload is more noticeable. Additionally, the steady-state thrust from the quadcopter positioned closest to the added payload is also higher in the sub-optimal setup. This suggests that, despite facing disturbances of the same magnitude, the thrust distribution becomes more uneven in the sub-optimal case, emphasizing the benefits of an optimal quadcopter layout. It is important to note that in the sub-optimal configuration, the model and controller gains were recomputed from scratch to maximize performances (i.e. we did not use the same controller as in the optimal configuration).

V. CONCLUSIONS

In this study, we introduced a novel approach to cooperative aerial transportation with a team of quadcopters, employing optimal control theory and a hierarchical control

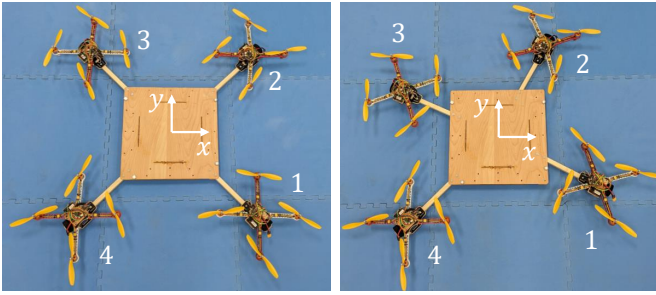


Fig. 6: Attachment layouts tested on panel B for disturbance rejection comparison. Left: optimal configuration, right: sub-optimal configuration.

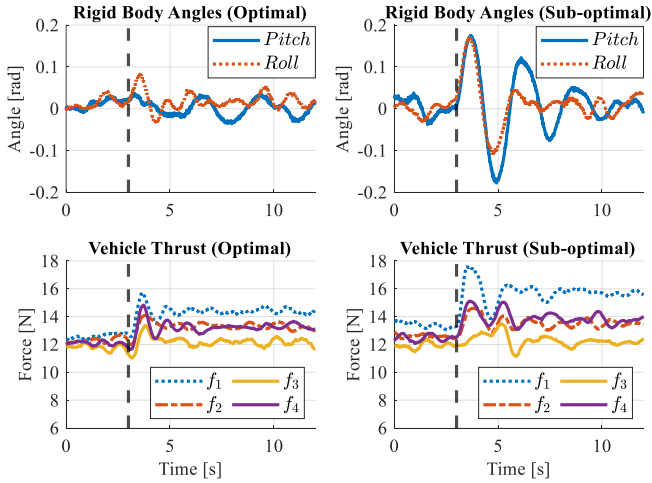


Fig. 7: Response to step disturbance over time. The mass is attached instantly (through a magnet) underneath Quadcopter 1. The attachment time is indicated with a vertical dashed line. On the top row, attitude response. On the bottom row, total quadcopter thrusts. Left: optimal configuration, right: sub-optimal configuration

strategy. This methodology offers an original approach in which the layout design and control problems are solved in a coupled way through an optimization routine derived from \mathcal{H}_2 control theory. Our optimization framework allows to cater our system to different payload shapes, inertias, and quadcopter counts. The hierarchical control structure offers a systematic and simple way to deal with the dynamics viewing the system as a single, integrated rigid body. The choice of the weight matrices C and D represents the freedom given to the control designer to obtain the desired performances. Overall, the main contributions of this paper are:

- An automated tool to optimally arrange thrust modules on a payload to maximize robustness of the integrated system;
- A control framework general enough to be able to fly different payload shapes and masses using the preferred number of quadcopters.

We also emphasize the idea that dealing with system design and control in a coupled manner simplifies the control complexity and increases the overall system performances compared to a sequential siloed approach (control design following system design).

Experimental results validate the effectiveness of our approach. Flight tests under disturbance highlighted the sta-

bility and robustness of the system, and, most importantly, the agreement between the performance predicted by our optimization tool and experimental evidence.

Future developments for this work include:

- Exploring more advanced control strategies and infrastructures. At this stage, for example, the vehicles' onboard sensor data were not used.
- Removing the assumption of known payload inertia and developing a control scheme under this uncertainty component.
- Using the system as a moving tray that can be used to transport and balance a payload placed on its top.

In conclusion, this study highlights the coupling between design variables and control. The physical placement of quadcopters significantly affects the performances of the controller. Optimizing the layout allows to take more advantage of optimal control tools rather than applying them at a second stage, once the design process is finished.

VI. ACKNOWLEDGMENTS

This work was funded by the Tsinghua-Berkeley-Shenzhen Institute (TBSI). The authors would also like to thank Roman Ibrahimov and Ruiqi Zhang for their precious help.

REFERENCES

- [1] D. K. Villa, A. S. Brandao, and M. Sarcinelli-Filho, "A survey on load transportation using multirotor uavs," *Journal of Intelligent & Robotic Systems*, vol. 98, pp. 267–296, 2020.
- [2] B. Arbanas, A. Ivanovic, M. Car, T. Haus, M. Orsag, T. Petrovic, and S. Bogdan, "Aerial-ground robotic system for autonomous delivery tasks," in *2016 IEEE international conference on robotics and automation (ICRA)*. IEEE, 2016, pp. 5463–5468.
- [3] J. Zeng, P. Kotaru, M. W. Mueller, and K. Sreenath, "Differential flatness based path planning with direct collocation on hybrid modes for a quadrotor with a cable-suspended payload," *IEEE Robotics and Automation Letters*, vol. 5, no. 2, pp. 3074–3081, 2020.
- [4] F. Schiano, P. M. Kornatowski, L. Cencetti, and D. Floreano, "Reconfigurable drone system for transportation of parcels with variable mass and size," *IEEE Robotics and Automation Letters*, vol. 7, no. 4, pp. 12 150–12 157, 2022.
- [5] S. Lee and H. Lee, "Trajectory generation of a quadrotor transporting a bulky payload in the cluttered environments," *IEEE Access*, vol. 10, pp. 31 586–31 594, 2022.
- [6] M. Moshref-Javadi and M. Winkenbach, "Applications and research avenues for drone-based models in logistics: A classification and review," *Expert Systems with Applications*, vol. 177, p. 114854, 2021.
- [7] G. Macrina, L. D. P. Pugliese, F. Guerriero, and G. Laporte, "Drone-aided routing: A literature review," *Transportation Research Part C: Emerging Technologies*, vol. 120, p. 102762, 2020.
- [8] M. W. Mueller, S. J. Lee, and R. D'Andrea, "Design and control of drones," *Annual Review of Control, Robotics, and Autonomous Systems*, vol. 5, no. 1, pp. 161–177, 2022.
- [9] H. Lee, H. Kim, and H. J. Kim, "Planning and control for collision-free cooperative aerial transportation," *IEEE Transactions on Automation Science and Engineering*, vol. 15, no. 1, pp. 189–201, 2016.
- [10] H. Lee, H. Kim, W. Kim, and H. J. Kim, "An integrated framework for cooperative aerial manipulators in unknown environments," *IEEE Robotics and Automation Letters*, vol. 3, no. 3, pp. 2307–2314, 2018.
- [11] C. Meissen, K. Klausen, M. Arcaç, T. I. Fossen, and A. Packard, "Passivity-based formation control for uavs with a suspended load," *IFAC-PapersOnLine*, vol. 50, no. 1, pp. 13 150–13 155, 2017.
- [12] H. Rastgoftar and E. M. Atkins, "Cooperative aerial lift and manipulation (calm)," *Aerospace Science and Technology*, vol. 82, pp. 105–118, 2018.

- [13] K. Mohammadi, M. Jafarinasab, S. Sirouspour, and E. Dyer, “Decentralized motion control in a cabled-based multi-drone load transport system,” in *2018 IEEE/RSJ International Conference on Intelligent Robots and Systems (IROS)*. IEEE, 2018, pp. 4198–4203.
- [14] J. Geng and J. W. Langelaan, “Implementation and demonstration of coordinated transport of a slung load by a team of rotorcraft,” in *AIAA Scitech 2019 Forum*, 2019, p. 0913.
- [15] D. Mellinger, M. Shomin, N. Michael, and V. Kumar, “Cooperative grasping and transport using multiple quadrotors,” in *Distributed Autonomous Robotic Systems: The 10th International Symposium*. Springer, 2013, pp. 545–558.
- [16] G. Loianno and V. Kumar, “Cooperative transportation using small quadrotors using monocular vision and inertial sensing,” *IEEE Robotics and Automation Letters*, vol. 3, no. 2, pp. 680–687, 2017.
- [17] K. Webb and J. Rogers, “Adaptive control design for multi-uav cooperative lift systems,” *Journal of Aircraft*, vol. 58, no. 6, pp. 1302–1322, 2021.
- [18] R. Ritz and R. D’Andrea, “Carrying a flexible payload with multiple flying vehicles,” in *2013 IEEE/RSJ International Conference on Intelligent Robots and Systems*. IEEE, 2013, pp. 3465–3471.
- [19] N. Bucki and M. W. Mueller, “A novel multicopter with improved torque disturbance rejection through added angular momentum,” *International Journal of Intelligent Robotics and Applications*, vol. 3, no. 2, pp. 131–143, 2019.
- [20] G. E. Dullerud and F. Paganini, *A course in robust control theory: a convex approach*. Springer Science & Business Media, 2013, vol. 36.
- [21] P. C. Mahalanobis, “On the generalized distance in statistics,” *Sankhyā: The Indian Journal of Statistics, Series A (2008-)*, vol. 80, pp. S1–S7, 2018.
- [22] J. A. Nelder and R. Mead, “A simplex method for function minimization,” *The computer journal*, vol. 7, no. 4, pp. 308–313, 1965.
- [23] J. C. Lagarias, J. A. Reeds, M. H. Wright, and P. E. Wright, “Convergence properties of the nelder–mead simplex method in low dimensions,” *SIAM Journal on optimization*, vol. 9, no. 1, pp. 112–147, 1998.